Explore the Potential of Air-Lift Pumps and Multiphase

Use this new capacity correlation for pump design.

F. A. Zenz,
AIMS

Applications of so-called "air-lift pumps" in fields other than petroleum (1) have included the handling of hazardous fluids (2), the design of bioreactors (3,4), the recovery of archeological artifacts (5), recycle aeration in sludge digestors (6), deep sea mining (7), and the recovery of manganese nodules (8,9,10) from ocean floors. Interest among a host of domestic (11-17,18) and foreign (19) organizations dates back several decades; having passed EPA hurdles (20), recovery of ocean resources has been further sanctioned by U.S. legislation (17). With the exception of "bioreactors" the practical design and operation of an air-lift pump lies in the dense-phase slug-flow regime of cocurrent gas-liquid upflow (21).

The transition to slug flow

The entrainment of spray or droplets as occurs from a fractionator tray constitutes a form of dilute phase cocurrent gas-liquid upflow. Since bubble caps have been used as foot pieces in gas lift pumps, a pipe set over a cap on a tray, as illustrated in Figure 1a, constitutes conceptually a low efficiency bubbling upflow gas lift operating at very shallow submergence. In practice, a gas lift operates with deeper submergence, and more efficiently in slug flow, as depicted in Figure 1b where the foot piece is simply a gas injection nozzle.

In practice, multiport injectors have been found to be more efficient (22) in terms of increased capacity, particularly in the bubbling and slug-flow regimes.

This is in accord with analogous experience in the injection of flashing feeds into risers in fluid catalytic cracking units, analogously carrying upwardly bulk solids (particles) as opposed to bulk liquids (molecules), and also accounts for some amount of scatter in published experimental data on air-lift capacity.

Since injected gas bubbles are displaced upwardly by the downward "slip" flow of liquid (that is, dense phase (23)) at the walls, the cross section through an upward moving gas bubble represents a countercurrent flow as depicted in Figure 1c despite a net upward transport of slugs of liquid. This local countercurrent flow is analogous to the empty pipe flooding phenomena illustrated in Figure 1d for which correlations already exist (24). In view of the identical flow phenomena in Figures 1c and 1d, accounting for the system variables should also be identical whether the net flows are cocurrent or countercurrent.

Dense phase liquid transport by gas-lift pumps

In Figure 1b, gas compressed to a pressure level equivalent to the depth of submergence is introduced to the lift pipe to displace liquid upwardly. As the liquid flows back down into the bubble-form-voids, more gas is continually introduced to establish a steady state of refluxing of upwardly displaced liquid. The net rate of conveyance or refluxing decreases with height of lift. If the pipe is cut off at some height, below the maximum commensurate with the given gas rate, or of the dif-
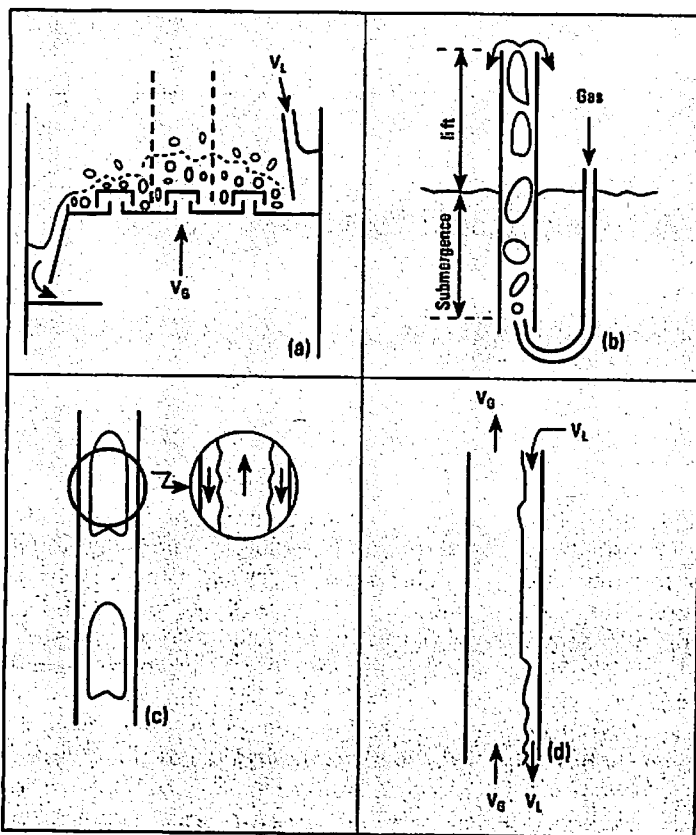
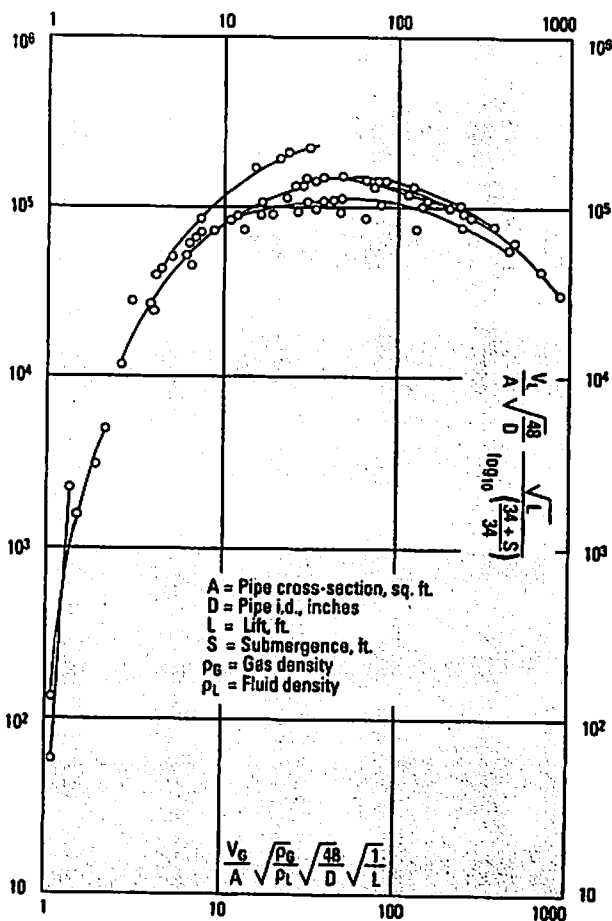■ *Figure 1. (above) Dilute-dense phase manifestations.*

■ *Figure 2. (right) "Correlation" of air-water lift data.*

ference in hydraulic head, then the net rate of liquid at that height will be continuously expelled from the pipe and hence the action referred to as a lift "pump."

Experimental air-lift data

Figure 2 displays a variety of published air-lift data covering lift heights ranging from 5 in. to 65 ft and pipe diameters from $\frac{1}{2}$ in. to 15 in. The curves drawn through each investigator's results fall into a numerical sequence with height of lift. The basis for the choice of coordinates in Figure 2 lays principally in their ability to correlate maximum countercurrent dilute phase-dense phase flow through empty vertical tubes and packed towers *(23,24)*. That these coordinates yield a plot as organized in Figure 2 lends credibility to this approach to correlation,

despite the fact that air lift represent overall a net cocurrent, rather than countercurrent, flow.

In Figure 2 gas volume and gas density are based on discharge conditions; within a long lift pipe these could vary significantly from inlet to discharge. However, the significance of "corrections" to the data in Figure 2 would be difficult to evaluate justifiably when even the best data are subject to experimental error and to the effects of the air injection arrangments *(22)*.

The submergence term, S, in the denominator of the ordinate of Figure 2 is based on analogy to correlating data on entrainment from distillation trays (25). It also reflects the work expanded in compressing the air in an air lift. If S is replaced by $\log [(S + 34)/34]$, which is proportional to the work of compression and still reflects the submergence,

then the data in Figure 2 yield a family of parallel curves spaced according to the square root of the lift height. Multiplying the ordinate and dividing the abscissa by the square root of L results in the correlation of Figure 2.

Effect of fluid density

Since all the data in Figure 2 are based on lifting water, the question arises as to how well this correlation would satisfy other fluids. The ordinate should be modified by considering that increased liquid density would logically result in reducing the effective volumetric yield, or conversely giving the same wieght yield at equal air rates. Chamberlain (2) obtained air-lift data for both water and a 93.5 lb/ft³ caustic solution in the same pipe; his data are plotted in Figure 3 and show excel-

lent correlation. Figure 3, which represents a smoothed band drawn through the data in Figure 2 may therefore be considered a more generalized correlation.

The Ingersoll-Rand equation

The theoretical efficiency of an air lift is simply the work required to lift the liquid to the point of discharge divided by the work of isothermal compression of the air. When analyzed in these terms, the air-to-liquid ratio can be expressed as a function of lift height, submergence, and efficiency. This relationship is generally recognized as the Ingersoll-Rand equation (26,27) and is usually accompanied with tabulated values of a constant derived from experimental data at or near the point of maximum efficiency of operation as a function of the lift height.

The work required to lift the dense phase (liquid) to the point of discharge is:

$$W_a = W_e L \qquad (1)$$

The work (isothermal compression) expended by the dilute phase (air) in lifting the liquid is:

$$W_I = P_a V_G \ln (P/P_a) \qquad (2)$$

and the fractional efficiency, E, is therefore:

$$E = W_a/W_I \qquad (3)$$

Since $P_a = 34$ ft of water or 14.7 psia, P may be expressed as $34 + S$, where S is the submergence in ft, so that

$$E = W_e L/P_a V_G \ln (P/P_a) \qquad (4)$$

(See Equations A, 5 and 6.) The published version of the Ingersoll-Rand equations is simply Eq. 6 with the term (469 E) replaced by a constant which in effect amounts to assigning a value to E. Operationally determined values of E are generally of the order of 40 to 50% at the point of maximum operating efficiency, as given in Table 1 (26).

From the Ingersoll-Rand equation

$$\frac{Abscissa}{of\,Figure\,4} = \frac{V_G \times 4 \times 144}{3.14\,(6)^2} \sqrt{\frac{0.0765}{62.4} \times \frac{48}{6} \times \frac{1}{30}} = 0.0916\,V_G$$

■ *Equation A*

$$\frac{V_G}{W_e} = \frac{L}{144 \times 14.7\,E \times \ln\,[(34+S)/34]}$$

■ *Equation 5*

$$\frac{(SCFM)_{Air}}{(GPM)_{Water}} = \frac{0.8\,L}{469\,E \times \log\,[(34+S)/34]}$$

■ *Equation 6*

$$\frac{(SCFM/ft^2)\,(48/D)^{1/2}}{(GPM/ft^2)\,(48/D)^{1/2}} = \frac{0.8\,L}{C \times \log\,[(34+S)/34]}$$
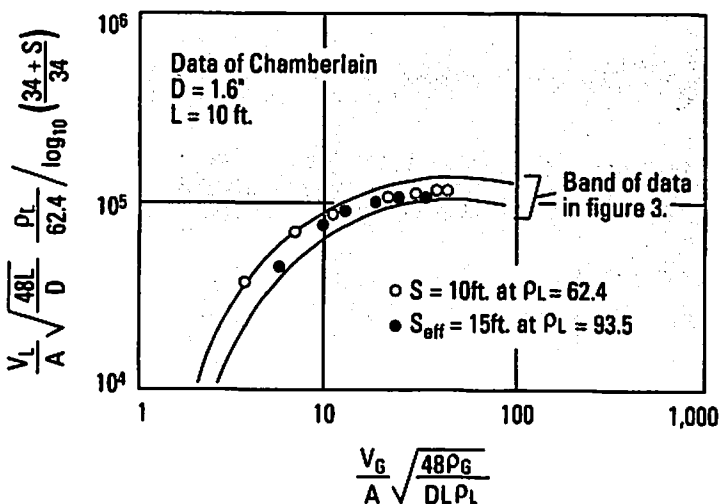
■ *Equation 7*

$$\frac{(V_G/A)\,(48/D)^{1/2}\,(\rho_d/\rho_L)^{1/2}/L^{1/2}}{(V_L/A)\,(48/D)^{1/2}\,L^{1/2}/\log\,[(S+34)/34]} = \frac{0.8\,(\rho_d/\rho_L)}{C}$$

■ *Equation 8*

alone, it is impossible to predict the variation in a given lift pipe's performance as air rates are changed. The equation gives the air-to-water ratio only at the point of peak efficiency and would imply that this ratio is constant at all air rates. It is evident from Figures 2 and 3 that the water rate falls off sharply when the air rate is either less (in the bubbling flow regime) or greater (in the annular or mist flow regime), than near the point of optimum slug-flow operation (28).

Multiplying numerators and denominators by equal terms, the Ingersoll-Rand equation can be rearranged for graphical comparison with Figures 2 and 3. From Eq. 6 see Eq.7 or Eq. 8. For standard air and
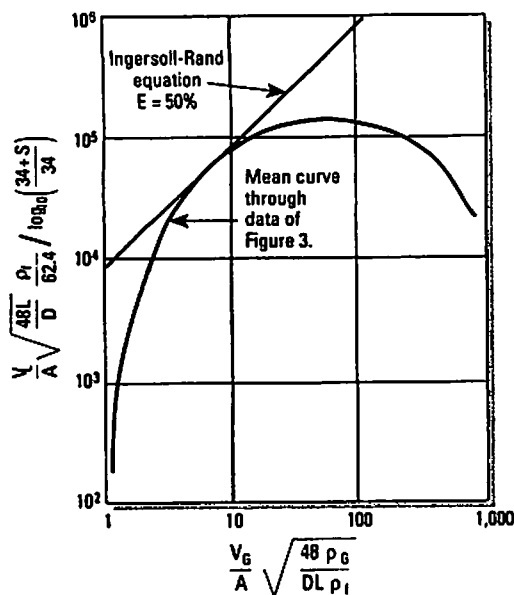

■ *Figure 3. Effect of fluid density.*

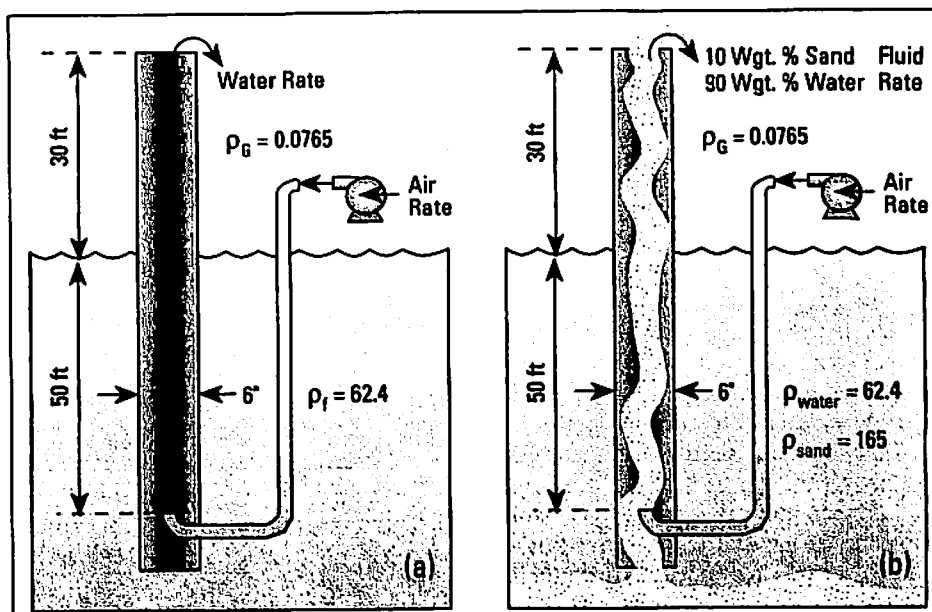■ *Figure 4. Significance of the Ingersoll-Rand equation.*

■ *Figure 5. Air-lift examples.*

Nomenclature

a	=	cross-sectional area of annular flow, sq. ft.
A	=	pipe cross-sectional area, sq. ft.
D	=	pipe inside diameter, in.
E	=	fractional efficiency, W_o/W_i
L	=	lift height, ft.
P	=	pressure at point of gas entry, lb/sq. ft.
P_a	=	atmospheric pressure, lb/sq. ft.
S	=	submergence, ft.
V_G	=	gas flow at discharge conditions, ft³/min
V_L	=	dense phase flow, gal/min
W_e	=	pounds of dense phase lifted per minute
W_i	=	work input ft-lb/min
W_o	=	work output ft.lb/min

Greek Letters

ε	=	gas void fraction in aerated dense phase
μ_f	=	viscosity of lifted fluid, entipoise
σ_f	=	surface tension of lifted fluid, dynes/cm
ρ_f	=	density of lifted fluid, lb/ft³
ρ_G	=	gas density, lb/ft³
ρ_L	=	liquid density, lb/ft³

water (that is, $\rho_L = 62.4$; $\rho_G = 0.0765$), Eq. 8 is then

$$\frac{0.028}{C} \qquad (9)$$

Equation 9 is shown in Figure 4 as superimposed on Figure 3. The Ingersoll-Rand equation plots as a straight line with slope corresponding to the air-to-water ratio at peak theoretical efficiency. The curve based on experimental data exhibits this same slope at only one point, but then curves away to yield lower water-to-air ratios at values of the abscissa (air rate) higher or lower than that corresponding to the ratio at this point of maximum delivery efficiency. The Ingersoll-Rand equation is therefore useful in estimating the yield from an air lift only under conditions of peak theoretical efficiency, but not over the entire range of possible operating conditions. Figures 3 and 4 incorporate as well the effect of fluids of densities other than water.
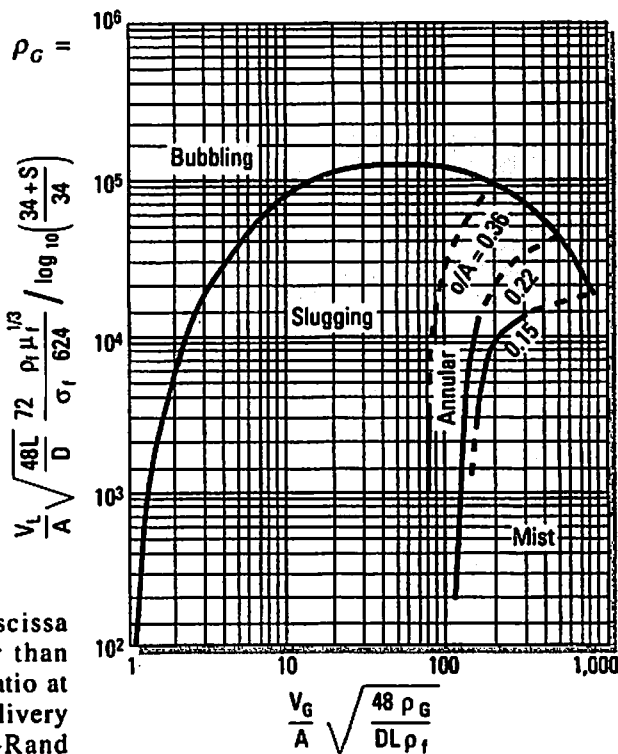

■ *Figure 6. Multiphase cocurrent vertical upflow regimes.*

Examples

Consider the operable gas-liquid-solids ratios for two situations illustrated in Figure 5:

1. Air lifting of water 30 ft through a 6 in. pipe submerged 50 ft.

$$\text{Equation B} \qquad \begin{array}{c}\text{Ordinate}\\ \text{of Figure 4}\end{array} = \frac{V_L \times 4 \times 144}{3.14\,(6)^2}\sqrt{\frac{48}{6}}\times\frac{(30)^{1/2}}{\log\,[(34+50)/34]} = 201\,V_L$$

$$\text{Equation C} \qquad \begin{array}{c}\text{Abscissa}\\ \text{of Figure 4}\end{array} = \frac{V_G \times 4 \times 144}{3.14\,(6)^2}\sqrt{\frac{0.0765}{66.5}\times\frac{48}{6}\times\frac{1}{33.1}} = 0.0844 \;(ACFM)$$

$$\text{Equation D} \qquad \begin{array}{c}\text{Ordinate}\\ \text{of Figure 4}\end{array} = \frac{(Slurry\,GPM)\times 4 \times 144}{3.14\,(6)^2}\sqrt{\frac{48}{6}}\;\frac{66.5}{62.4}\times\frac{(33.1)^{1/2}}{\log\,[(34+46.9)/34]} = 235\;(Slurry\,GPM)$$

2. Air lifting of a sedimented sand, as a slurry containing 10 wt.% fine sand, a distance of 30 ft through a 6 in. pipe submerged 50 ft.

Case 1.
See Eqs. A, B and Table 2.
Case 2.

Slurry density $= 1/[(0.1/165) + (0.9/62.4)]$
$\qquad\quad = 66.5\;lb/ft^3$

Effective submergence $=$
$50\,(62.4/66.5) = 46.9$ ft.
Effective Lift $= 30 + 50 - 46.9 = 33.1$ ft.
See Eqs. C, D and Table 3.

Bubbling and annular liquid flow

At values of the abscissa less than about 50 and to the left of the curve in Figure 4, two-phase flow would occur in the form of gas bubbles rising in a matrix of liquid forced to flow upwardly by means, for example, of a motor driven pump or simply by a hydraulic difference in head. Under such conditions, typical in bioreactors *(3)*, L would be the tube diameter and S would equal

$$L\rho_f (1-\varepsilon)/62.4$$

At values of the abscissa greater than about 50, and to the right of the curve in Figure 4, voidage must be so great that liquid can only be driven up the pipe in annular flow by the surface drag of the gas core. This region has been explored in some detail by Dukler and others *(29,30)*

Table 1. Operationally determined values of E, that is, fractional efficiency.

Lift (ft)	E in Eq. 6	489 E, the constant C in the Ingersoll-Rand equation
10-60	0.52	245
61-200	0.50	233
201-500	0.46	216

Table 2. Air rates and water lifted for Case 1.

V_G Air Rate (ACFM)	Figure 4 Abscissa	Ordinate	V_L Water Lifted (gpm)
50	4.58	37,000	184
80	7.33	65,000	323 ← peak efficiency
100	9.16	76,000	378
200	18.32	112,000	557
400	36.64	139,000	692
800	73.29	140,000	696 ← peak delivery
1,000	91.60	133,000	661
2,000	183.20	103,000	513

Table 3. Air rates and water lift rates for Case 2.

Air Rate ACFM	Figure 4 Abscissa	Ordinate	GPM Mix	Lift Rates Water lb/h	Sand lb/h
50	4.22	39,000	140	67,230	7,470
100	8.44	70,000	298	143,000	15,880 ← Peak E%
200	16.88	109,000	464	222,750	24,750
400	33.76	136,000	578	278,000	30,880
800	67.52	141,000	600	288,000	32,000 ← Peak Delivery
1,000	84.40	138,000	587	282,000	31,300
2,000	168.80	108,000	460	221,000	24,530

who presented experimental data relating measured amounts of liquid, carried upward in annular films of measured thickness inside a vertical 2 in. internal diameter (ID) pipe, to the measured rate of the cocurrent, liquid flow inducing, upward gas stream.

The results are shown in Figure 6 with the ratio of film cross-sectional area to pipe cross-sectional area as a parameter. Equating bubble rise velocity to displacing liquid downflow in a slugging tube, corresponds to an annulus-to-tube area ratio of 0.385, suggesting that these investigators were approaching slugging and that this limit should at some time be established on Figure 6 experimentally. The addition of liquid viscosity and particularly surface tension terms to the ordinate of Figure 6 has been, somewhat arbitrarily, based on identical terms applicable to horizontal multiphase flow *(31)* and on data obtained for very low surface tension liquids in cocurrent upflow with air *(32)* in tubes several in. to several ft in diameter.

Figure 6 represents not only a capacity correlation for gas lift pump design, but also suggests the correlation of all regimes of cocurrent multiphase upflow to the extent supported by data published to date. **CEP**

Literature Cited

1. Brown, K. E., "Gas Lift Theory and Practice," Pet. Publishing Co., Tulsa, Oklahoma (1973).
2. Chamberlain, H. V., AEC Idaho Operations Report No. 14398 (March 18, 1957).
3. Chisti, Y., "Assure Bioreactor Sterility," 88(9), Chem. Eng. Progress, pp. 80-85 (Sept. 1992).
4. Chisti, Y., and M. Moo-Young, "Improve the Performance of Airlift Reactors," Chem. Eng. Progress (June 1993).
5. Peterson, M., Oceanology International, pp. 34, 35 (July-Aug. 1968); pp. 16, 17 (Sept.-Oct. 1967).
6. Chem. Eng., pp. 58, 60 (Dec. 18, 1967).
7. McIlhenny, W. F., Chem. Eng., pp. 247-254 (Nov. 7, 1966).
8. Menard, H. W., Amer. Scientist, pp. 519-529 (Sept.-Oct. 1976).
9. Mero, J. L., Chem. Eng., pp. 73-80 (July 1, 1968).
10. Sorem, R. K., and R. H. Fewkes, "Manganese Nodules," Plenum Publishing, New York (1979).
11. Chem. & Eng. News, p. 17 (Jan. 18, 1965).
12. Chem. & Eng. News, p. 25 (Jan. 25, 1965).
13. Chem. & Eng. News, p. 13 (Aug. 31, 1990).
14. Chem. & Eng. News, p. 9 (Dec. 4, 1972).
15. Chem. & Eng. News, p. 19 (Feb. 11, 1974).
16. Chem. & Eng. News, p. 19 (April 10, 1978).
17. Chem. & Eng. News, p. 14 (July 7, 1980).
18. N. Y. Daily News, p. 69 (Jan. 4, 1976).
19. Chem. Week, pp. 33-34 (July 30, 1980).
20. Chem. Eng., p. 20 (Nov. 3, 1980).
21. Padan, J. W., "The Air Lift Mining Research Program," U. S. Bureau of Mines, Tiburon, CA (May 1965).
22. Morrison, G. L., et al., I & E C Res., 26, 387-391 (1987).
23. York, J. L., et al., "Solve All Column Flows With One Equation," Chem. Eng. Progress, 88(10), pp. 93-98 (Oct. 1992).
24. Zenz, F. A., and R. E. Lavin, Hydrocarbon Processing, 44(3), pp. 121-126 (1965).
25. Schweitzer, P. A., Handbook of Separation Techniques for Chemical Engineers, McGraw-Hill, New York pp. 3-86 to 3-88 (1988).
26. "Chemical Engineer's Handbook," 4th ed., McGraw-Hill pp. 6-13, (1963) derived in Ingersoll-Rand Bulletin (July 1929).
27. Duckworth, C. L., Chem. Proc., p. 63 (March 1960).
28. Nemet, A. G., Ind. Eng. Chem., 53(2), pp. 151-154 (1961).
29. Zabaras, G., et al., "Vertical Upward Cocurrent Gas-Liquid Annular Flow," AIChE J., 32(5), pp. 829-843 (1986).
30. Taitel, Y. et al., "Modelling Flow Patterns Transitions for Steady Upward Gas-Liquid Flow in Vertical Tubes," AIChE J., 26(3), pp. 345-354 (1980).
31. Baker, O., Oil & Gas J., pp. 185, 195, 53(12) (July 26, 1954).
32. Zenz, J. A., personal communication, PEMM Corp., Cold Spring, NY (1986).